

Article

## Deprotection-induced morphology transition and immuno-activation of glyco-vesicles: a strategy of smart delivery polymersomes

Wenjing Qi, Yufei Zhang, Jue Wang, Guoqing Tao, LIBIN WU,  
Zdravko Kočovski, Hongjian Gao, Guosong Chen, and Ming Jiang

*J. Am. Chem. Soc.*, **Just Accepted Manuscript** • DOI: 10.1021/jacs.8b04731 • Publication Date (Web): 18 Jun 2018

Downloaded from <http://pubs.acs.org> on June 24, 2018

### Just Accepted

“Just Accepted” manuscripts have been peer-reviewed and accepted for publication. They are posted online prior to technical editing, formatting for publication and author proofing. The American Chemical Society provides “Just Accepted” as a service to the research community to expedite the dissemination of scientific material as soon as possible after acceptance. “Just Accepted” manuscripts appear in full in PDF format accompanied by an HTML abstract. “Just Accepted” manuscripts have been fully peer reviewed, but should not be considered the official version of record. They are citable by the Digital Object Identifier (DOI®). “Just Accepted” is an optional service offered to authors. Therefore, the “Just Accepted” Web site may not include all articles that will be published in the journal. After a manuscript is technically edited and formatted, it will be removed from the “Just Accepted” Web site and published as an ASAP article. Note that technical editing may introduce minor changes to the manuscript text and/or graphics which could affect content, and all legal disclaimers and ethical guidelines that apply to the journal pertain. ACS cannot be held responsible for errors or consequences arising from the use of information contained in these “Just Accepted” manuscripts.

# Deprotection-induced morphology transition and immuno-activation of glyco-vesicles: a strategy of smart delivery polymersomes

Wenjing Qi<sup>†</sup>, Yufei Zhang<sup>†</sup>, Jue Wang<sup>†</sup>, Guoqing Tao<sup>†</sup>, Libin Wu<sup>†</sup>, Zdravko Kochovski<sup>‡</sup>, Hongjian Gao<sup>¶</sup>, Guosong Chen<sup>\*†</sup> and Ming Jiang<sup>†</sup>

<sup>†</sup>The State Key Laboratory of Molecular Engineering of Polymers and Department of Macromolecular Science, Fudan University, Shanghai, 200433 China

<sup>‡</sup> Soft Matter and Functional Materials, Helmholtz-Zentrum Berlin für Materialien und Energie, 14109 Berlin, Germany

<sup>¶</sup> Department of Electron Microscopy, School of Basic Medical Science, Fudan University, Shanghai, 200032 China

**KEYWORDS:** *Deprotection, Responsive polymersome, Glycopolymer, Morphology transition, Antigen presentation*

**ABSTRACT:** We proposed the deprotection-induced block copolymer self-assembly (DISA), that is, the deprotection of hydroxyl groups resulted in *in situ* self-assembly of glycopolymers. In the previous studies, block copolymers soluble in common organic solvents were employed as the starting material. In this paper, by using the protected glyco-block containing pre-assembled glyco-vesicles in water as the starting material, we moved forward and made two exceeding achievements. Firstly, we have observed a deprotection-induced morphology transition triggered by alkali in water. The carbohydrate-carbohydrate interaction was considered to contribute to such a morphology transition during deprotection. Secondly, lipase was found to be an efficient enzymatic trigger in the sugar deprotection, which motivates the immune-application of this morphology transition process. When lipase and a model antigen, ovalbumin (OVA), were encapsulated inside the glyco-vesicles, the deprotection of sugars by lipase induced the transition of vesicles to micelles and the lipase and OVA were released accordingly. When glyco-vesicles were internalized by dendritic cells (DCs), the lipase from lysosomes efficiently induced the release of OVA and presentation of antigen to T cells. During the process, lysosomal lipase performed as a trigger on the deprotection of sugars and the release of protein without any other reagents. The significance of this design is that as a delivery vehicle, the protected glyco-vesicles not only avoided unnecessary immune activation, but also worked with the released OVA together, i.e. the glyco-vehicle successfully activated DCs and improved presentation efficiency of T cells remarkably.

## INTRODUCTION

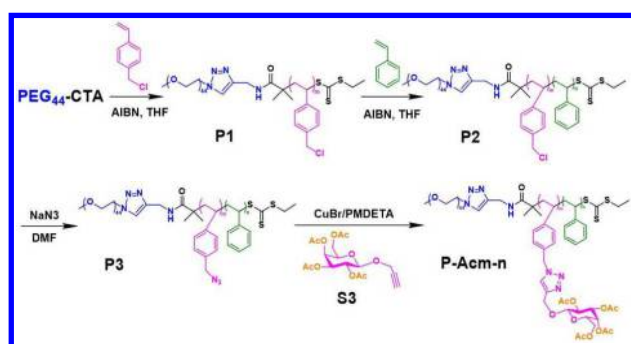
Responsive polymersomes, as attractive biomimetic candidates of cellular compartments, are capable of responding to various stimuli by extensive tailored designs.<sup>1</sup> Highlighted with tunable membrane properties, e.g. robustness and permeation, as well as the capacity of transporting hydrophilic/hydrophobic species, responsive polymersomes exhibit promising applications as drug delivery vehicles, diagnostic reagents, nano-reactors and artificial organelles.<sup>2</sup> Several triggers including temperature,<sup>3</sup> pH,<sup>4</sup> light,<sup>5</sup> ultrasound,<sup>6</sup> magnetic field,<sup>7</sup> oxidation,<sup>8</sup> redox,<sup>9</sup> and enzymes<sup>10,11</sup> have been employed to induce the responsiveness. However, in most cases after delivery, the polymersomes themselves usually fall apart without any functions which to our point of view is not atom-economic and might induce some side effects in the real bio-applications. Thus, it is demanding to activate the delivery polymersome after triggered release. Herein, activation means not only the encapsulated molecules are released but also the container itself can obtain some additional functions as a "new" nano-object and works with the released drug together.

Sugars on the cell surface participate in various biological events, including cell-cell adhesion, cell recognition, and cell differentiation by binding to external receptors through carbohydrate-protein interactions.<sup>12</sup> When sugars bind to receptors on immune cell surfaces, the cells are stimulated with high expression of certain signaling molecules and high secretion of cytokines.<sup>13</sup> Glycopolymers, a nice mimic to native glycans, has been proved to induce the cross-linking of lectins which control the cell functions and signal transduction.<sup>14</sup> Thus we expect sugar-containing polymersomes to be activated and will perform their functions with the drug together when they are used as drug-delivers. Recently, we introduced the deprotection-induced self-assembly of glycopolymer, i.e. deprotection of pendent sugars induced the self-assembly of glycopolymers *in situ*, resulting in the formation of micelles or vesicles.<sup>15</sup> To our opinion, the deprotection process changed the bio-inactive protected sugars to bio-active free ones, which may boost the response of immunological cells and is consistent to the idea of activation highlighted in this paper.

Herein, we report a new type of polymersome, prepared by protected pendant carbohydrate units containing block copolymers. Triggered by deprotection chemistry, the polymersomes transformed to other morphologies with larger sizes and aggregation numbers. The phenomenon was quite unusual when compared to previously reported polymersomes disintegration,<sup>16</sup> and was attributed to carbohydrate-carbohydrate interactions after deprotection. Both alkali and enzyme could be employed as deprotection reagents to trigger the morphology transition in water. In the case of enzymatic deprotection, the process can also be achieved in cellular lysosomal compartments, where lipase exists as a natural trigger.<sup>17,18</sup> When a model antigen OVA was encapsulated in the sugar-containing vesicles, it was released slowly to activated DCs and then boosted the response of immune cells. We demonstrate that T cells were activated more efficiently by OVA-loaded glyco-vesicles than OVA itself via improved antigen uptake and presentation process, and these results can prove that the glyco-vesicles were activated during the deprotection-induced antigen release.

### Scheme 1. Synthetic routes of triblock glycopolymer P-

Acm-n.



## RESULTS AND DISCUSSION

**Design and synthesis of triblock glycopolymers P-Acm-n.** To achieve the desired polymersomes in water, triblock copolymers which possess hydrophilic poly (ethylene glycol) (PEG) block, protected sugar block and hydrophobic polystyrene (PS) block were prepared via RAFT polymerizations and post-polymerization modification (Scheme 1). PEG was selected to stabilize the assembled copolymers in solution, while PS was chosen due to its high electron contrast under microscope for morphology observation. The middle sugar block was designed to induce deprotection-induced morphology transition. Galactose was chosen because of the abundant galactose receptors on cell surfaces, which could play important roles in mediation of immune activation in cellular process. The corresponding triblock copolymers were named **P-Acm-n** for clarity (**P**: PEG; **Acm**: acetyl protected sugar block with **m** as the degree of polymerization (DP); **n**: DP of PS block). Four different copolymers **P-Ac50-36**, **P-Ac100-60**, **P-Ac100-140**, **P-Ac100-350** with low dispersities were prepared and their characterization details are given in the supporting information (Figure Si-9). A list of molecular weights measured by <sup>1</sup>H NMR and the absolute molar masses determined by SEC-MALS (Size

Exclusion Chromatography with Multi-angle Light Scattering detector) were summarized in Table 1.

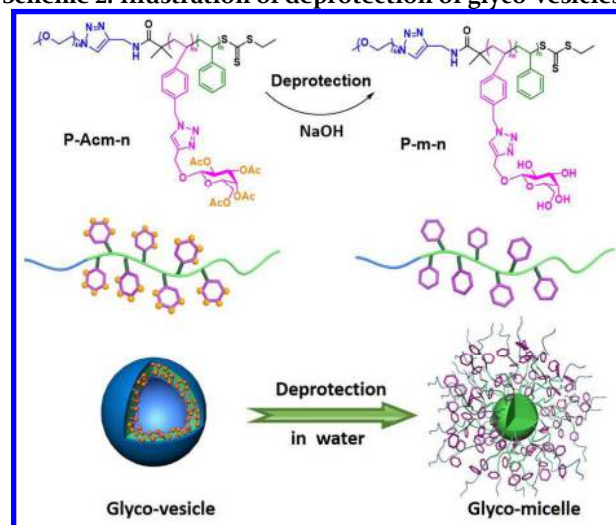
**Preparation and deprotection of glyco-vesicles.** The self-assembly of **P-Acm-n** was firstly performed via conventional solvent switch method.<sup>19</sup> Briefly, copolymers were dissolved in THF, followed by the addition of water. And then the solution was dialyzed against water to remove any organic solvent. As designed, these four copolymers all self-assembled into well-dispersed vesicles, which are characterized by Transmission Electron Microscopy (TEM) (Figure 1a and 3) and Dynamic Light Scattering (DLS) (Figure 1b), and the results were summarized in Table 2. These vesicles formed by protected sugars are name as *glyco-vesicles* in this paper.

**Table 1. Characterization of P-Acm-n.**

polymer	$M_n^a$ (kDa)	$M_w^b$ (kDa)	$M_n^b$ (kDa)	$\bar{D}$
P-Ac50-36	33.3	53.3	42.2	1.26
P-Ac100-60	61.2	82.1	59.1	1.38
P-Ac100-140	71.3	119.0	96.3	1.24
P-Ac100-350	93.2	124.7	88.6	1.40

<sup>a</sup>Number-average molecular weight ( $M_n$ ) was determined by <sup>1</sup>H NMR. <sup>b</sup>Number-average molecular weight ( $M_n$ ), weight-average molecular weight ( $M_w$ ), and polydispersity index ( $\bar{D}$ ) were measured by SEC-MALS.

### Scheme 2. Illustration of deprotection of glyco-vesicles.



Then the deprotection reaction was performed on these vesicles directly (Scheme 2). In our previous study, the deprotection of acetyl groups was performed in THF and tetrabutylammonium hydroxide was used as the base.<sup>15</sup> However, in the current study, the deprotection will be performed in aqueous media, where vesicles were formed. NaOH was used due to the high solubility in water and deprotection efficiency when compared to other reagents. After deacetylation, the four copolymers are represented as **P-50-36**, **P-100-60**, **P-100-140**, **P-100-350** and therefore the initial Ac is removed.

The efficiency of deacetylation on these vesicles by NaOH was firstly confirmed by <sup>1</sup>H NMR analysis. For example, vesicle solution of **P-Ac50-36** (10 mg/mL) was treated with NaOH and then dialyzed (MWCO 3500) against water to

remove free acetic acid before lyophilization for  $^1\text{H}$  NMR characterization. As shown in Figure 1c, after adding 10 equiv. of NaOH (according to the mole of Ac groups) into the vesicle solution, the intensity of Ac signals was significantly reduced, while only 10% of them still remained. If 30 equiv. of NaOH was added, the peaks of acetyl groups almost disappeared (only 4% remained) after 3 days, showing the successful removal of acetyl groups in glyco-vesicles. Further addition of NaOH did not result in higher removal ratio of Ac groups, showing a maximum deprotection degree when deprotection was performed in water. Compared to glycopolymers existing as unimers in THF, glyco-vesicles showed longer deprotection time (3 days) for near full deprotection since the protected glyco-blocks were embedded in vesicle walls, which retarded the reaction efficiency of NaOH.

Interestingly, TEM analysis after deprotection revealed a morphology transition from vesicles to micelles (Figure 1a). The  $\langle R_g \rangle$  (Radius of Gyration)/ $\langle R_h \rangle$  (Hydrodynamic Radius) value of the assemblies of **P-50-36** was measured by using Static Light Scattering (SLS) and DLS, and were found to decrease from 0.95 to 0.78 after deprotection (Table 2). The change in  $\langle R_g \rangle / \langle R_h \rangle$  value was consistent to the morphology transition from vesicles to micelles. This transition is in accordance to what expected from the packing parameter or the well-known H/L ratio (DP ratio of hydrophilic to hydrophobic blocks),<sup>19,20</sup> because the deprotection has turned the hydrophobic sugar blocks into hydrophilic ones. Surprisingly, a significant increase in  $\langle R_h \rangle$  from 61 nm to 103 nm was detected by DLS (Figure 1b). In literature, the most reported vesicle-to-micelle transition processes were often accompanied by a decrease in  $\langle R_h \rangle$  due to the collapse and disassembly of vesicles.<sup>21</sup> As the significant increase of  $\langle R_h \rangle$  observed in **P-Ac50-36** is unexpected, it inspires us to explore more on the mechanism of deprotection-induced morphology transition.

**Mechanism of deprotection-induced morphology transition.** The aggregation number ( $N_{agg}$ ) of the assemblies was measured by SLS. By comparing the  $N_{agg}$  values of the four assemblies before and after deprotection (Table 2), we found that this process was not a simple vesicle collapse but accompanied by a significant increase in  $N_{agg}$ . It indicated that the fusion of vesicles took place during the morphology transition process. As shown in the  $\langle R_h \rangle$  evolution profile (Figure 2a), upon the addition of NaOH,  $\langle R_h \rangle$  increased dramatically in the first 8 h to a maximum at 130 nm and then decreased to a plateau around 103 nm after 30 h. The shape transition can be better understood by tracing the morphology evolution under TEM (Figure 2b). Larger assemblies with a diameter around 300 nm were observed after 8 h, which was consistent to the DLS results. These large assemblies exhibited loose structures as a result of fusion of several smaller assemblies. Then, a relatively stable state with decreased surface tension was achieved with the formation of smaller and

more compact micelles with a diameter around 200 nm after 72 h. We can deduce that instead of the vesicle collapse mechanism, the disintegrated vesicles in this state underwent a fusion mechanism leading to larger assemblies and then reorganized to form more compact micelles. Obviously, the aggregation of the disintegrated vesicles played a significant role in the radius increase, indicating the existence of strong fusion interactions after exposure of sugars. Herein, we propose that the strong fusion is mainly caused by carbohydrate-carbohydrate interactions<sup>22</sup> (CCI) due to the exposure of large amounts of hydroxyl groups after removal of acetyl groups.

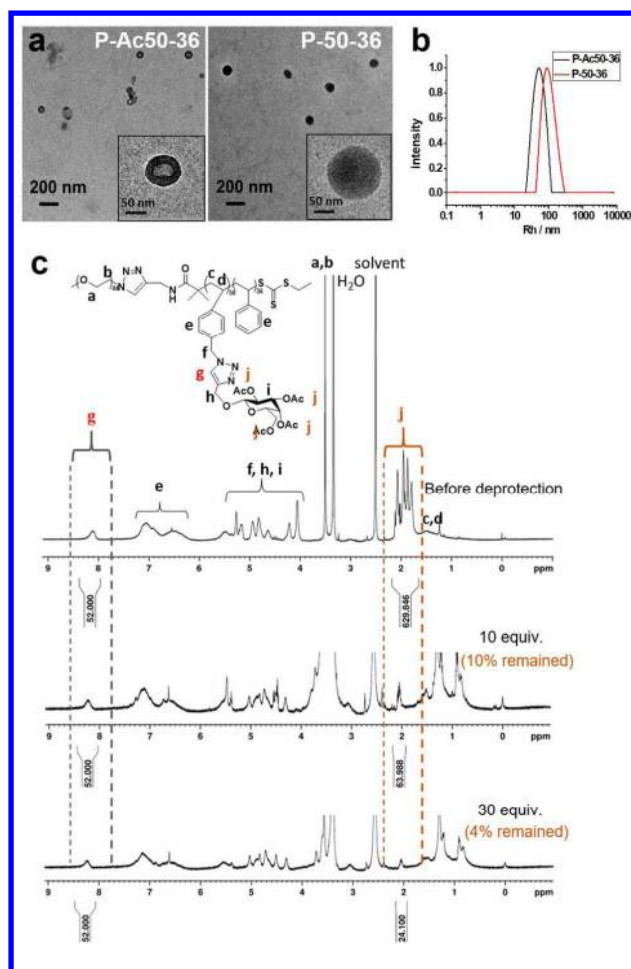


**Figure 1.** (a) TEM images (insets: images in higher magnification) and (b)  $\langle R_h \rangle$  distributions of **P-Ac50-36** before and after deprotection. TEM samples were prepared without staining. (c)  $^1\text{H}$  NMR spectra of **P-Ac50-36** in DMSO- $d_6$  after addition of different amounts of NaOH (10 and 30 equiv. to acetyl groups).

**Table 2. Summary of  $\langle R_h \rangle$ ,  $\langle R_g \rangle$  values and morphology transitions.**

polymer	$\langle R_h \rangle$ /nm	PDI	$\langle R_g \rangle$ /nm	$\langle R_g \rangle / \langle R_h \rangle$	$N_{agg}$	Morphology <sup>a</sup>	H/L <sup>b</sup>
P-Ac50-36	61	0.10	58	0.95	113	V	0.51
P-50-36	103	0.10	80	0.78	385	M	2.61
P-Ac100-60	128	0.07	150	1.17	1818	V	0.28

P-100-60	116 <sup>c</sup>	0.10 <sup>c</sup>	176 <sup>c</sup>	1.52 <sup>c</sup>	1236 <sup>c</sup>	S	2.40
P-Ac100-140	65	0.08	65	1.00	110	V	0.18
P-100-60	98	0.11	75	0.77	1613	M	1.03
P-Ac100-350	100	0.06	118	1.18	2833	V	0.10
P-100-350	170	0.12	210	1.23	8840	C-M	0.41

<sup>a</sup>V: vesicle; M: micelle; S: lamella sheet; C-M: compound micelle.

<sup>b</sup>H/L is the ratio of DP (hydrophilic) / DP (hydrophobic).

<sup>c</sup>lamellar structures may not be suitable for light scattering characterization.

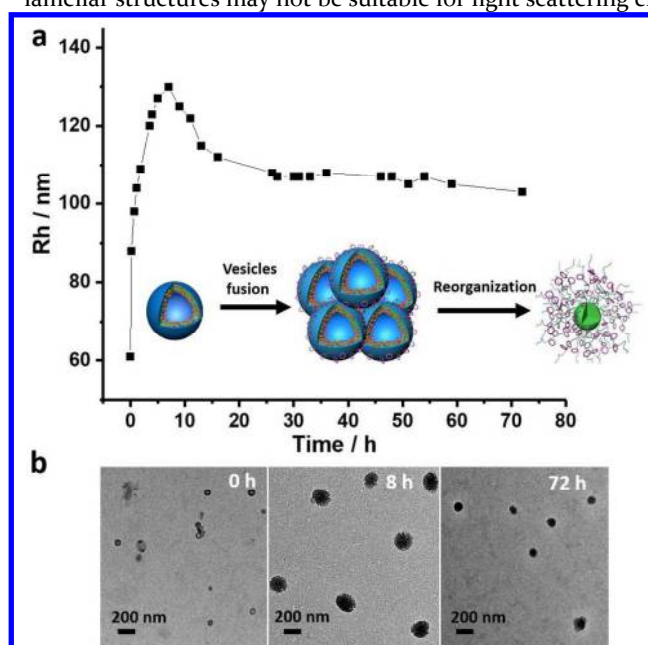


**Figure 2.** Schematic presentation of the proposed mechanism of deprotection-induced morphology transition. (a) Evolution of  $\langle R_h \rangle$  during the deprotection process starting from the addition of NaOH to the assembly of P-Ac50-36. (b) TEM images showing nano-structures of P-Ac50-36 after addition of NaOH for 0 h, 8 h and 72 h, when vesicles, fused vesicles and micelles were observed respectively.

It is known that CCI could be mediated by  $\text{Ca}^{2+}$  which causes the association of saccharides.<sup>23</sup> To confirm CCI,  $\text{Ca}^{2+}$  was added in the deprotection process at three different time points and obvious association of micelles was visualized and characterized by using DLS and TEM analysis (Figure S11). In order to have a better insight on the CCI during this process, vesicles self-assembled from P-Ac100-60, P-Ac100-140 and P-Ac100-350 with different sugar contents (50%, 35% and 20% respectively, mol%) were further studied (Figure 3). After the same deprotection procedure with P-Ac50-36, P-Ac100-140 vesicles also transformed to micelles while P-Ac100-60 vesicles changed to cylinder micelles and P-Ac100-350 vesicles to compound micelles (Figure 3, Table 2). Both vesicles from P-Ac100-60 and P-Ac100-140 were expected to transform to spherical micelles as P-Ac50-36 did if the morphological transitions were mainly governed by H/L ratio, since P-100-60 and P-100-140 have higher H/L ratios than 0.5 (Table 2). However, P-100-60 generated lamella sheets instead of spherical micelles although it shared a similar H/L ratio with P-50-36. We think this morphology difference was attributed to the difference in sugar block contents. The relatively higher contents of sugars led to stronger CCI, making

the entanglement between hydrophilic chains more intense during the fusion process than the polymers with lower sugar contents, leading to the formation of lamella sheets, which was further confirmed by Cryo-EM analysis (Figure S13). The CCI was also effective in the case of P-100-350, which was expected to adopt vesicular shape after deprotection, but transformed into compound micelles due to the increased chain entanglements. Only P-100-140 showed similar morphologies with P-50-36 sharing similar sugar block contents.

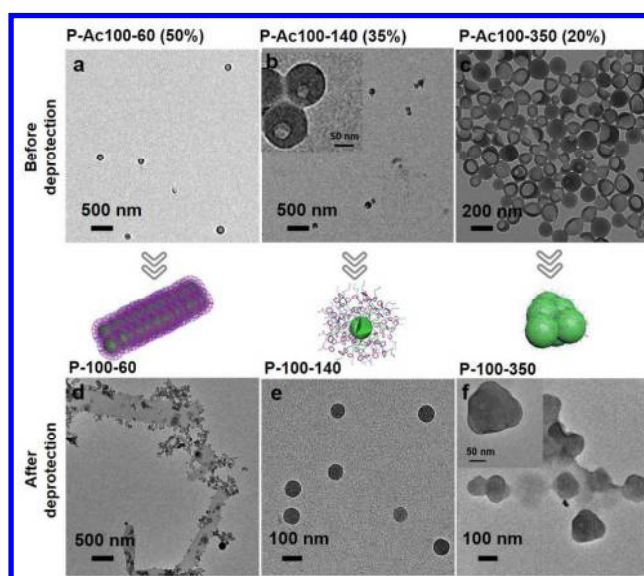


**Figure 3.** TEM images showing the varied morphologies of different glyco-vesicles after deprotection reactions: P-Ac100-60 vesicles (a) changed to P-100-60 lamella sheets (d), P-Ac100-140 vesicles (b) transformed to P-100-140 micelles (e) while P-Ac100-350 vesicles (c) changed to P-100-350 compound micelles (f) respectively.

**Lipase-catalyzed deprotection of glyco-vesicles.** We are curious to explore biological functions and applications of this deprotection-induced morphology transition since acylation indeed is a natural modification to proteins, saccharides and lipids with biological signaling mechanism.<sup>24</sup> To this goal, firstly we have to replace the inorganic base with enzymes in order to perform deprotection under physiological conditions. Lipase is a family of enzymes that catalyze the hydrolysis of lipids and performs essential roles in digestion, transportation and processing of dietary lipids.<sup>25</sup> After comparison of different lipases, lipase type I from wheat germ was chosen due to the high efficiency for deprotection-induced morphology transition. A model reaction of lipase-catalyzed deprotection of D-galactoside pentaacetate was conducted and confirmed by Thin-layer Chromatography

(Figure S14). Considering that **P-Ac50-36** follows the typical vesicle-to-micelle transition and also has the shortest PS block, which is more biological friendly in the following biological investigations, **P-Ac50-36** was focused on to explore biological functions and applications. Successful deprotection of **P-Ac50-36** vesicles with the addition of lipase in water with neutral pH was also characterized by  $^1\text{H}$  NMR (Figure S15). The morphology transition was also traced by DLS (Figure S16) and TEM (Figure 4), showing that lipase-catalyzed deprotection has a similar mechanism to NaOH-catalyzed ones with vesicle-to-micelle transition. Larger assemblies were also observed at the beginning by vesicles fusion and confirmed by using Cryo-EM analysis. (Figure S17)

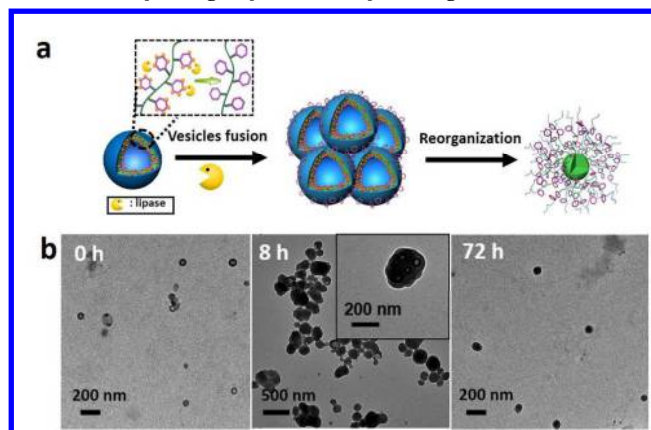


**Figure 4.** (a) Schematic presentation of the proposed mechanism of lipase catalyzed deprotection-induced morphology transition. (b) TEM images showing nano-structures of **P-Ac50-36** after addition of lipase for 0 h, 8 h and 72 h, when vesicles, fused vesicles and micelles were observed respectively.

**Lipase self-release via the encapsulation into glyco-vesicles.** Polymersomes can be turned into nanoreactors by encapsulating active enzymes.<sup>10,11</sup> Interestingly, when lipase was captured inside **P-Ac50-36** polymersomes, it can be self-released gradually without any stimuli or changes in external environment (Figure 5a). The process continued for 60 h till 90% of lipase was released (Figure 5b and Figure S20). By comparing lipase release profile with the  $\langle R_h \rangle$  evolution curve, it was found that in the first 30 h, significant change of  $\langle R_h \rangle$  and more than 60% release of lipase were observed, indicating that the morphology transition was accompanied by the release of lipase.

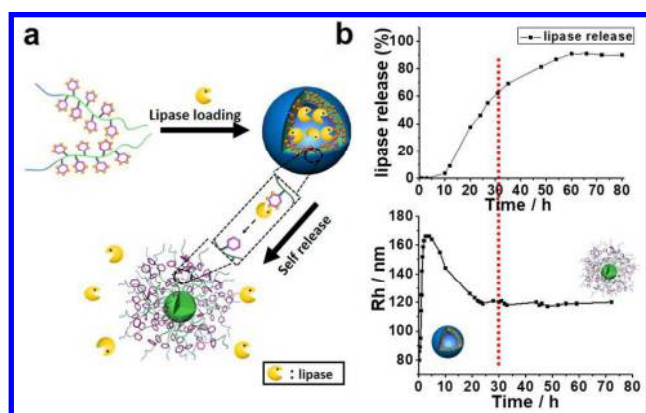


**Figure 5.** (a) Schematic representation of lipase self-release via the deprotection of **P-Ac50-36** glyco-vesicles. (b) Release profile (%) of lipase and  $\langle R_h \rangle$  evolution curve of glyco-vesicles via the deprotection reaction.

Furthermore, we utilized the enzymatic responsive polymersomes to release protein drugs (Figure 6a). FITC-labeled ovalbumin (OVA) was encapsulated together with lipase. The release of OVA was monitored by time-dependent fluorescence at 519 nm (Figure 6b,c). The results showed that 90% of OVA was released within 70 h. Meanwhile, the color of vesicle solutions collected from dialysis tube change from light-yellow to colorless, indicating successful release of FITC-labeled OVA after deprotection (Figure 6d).

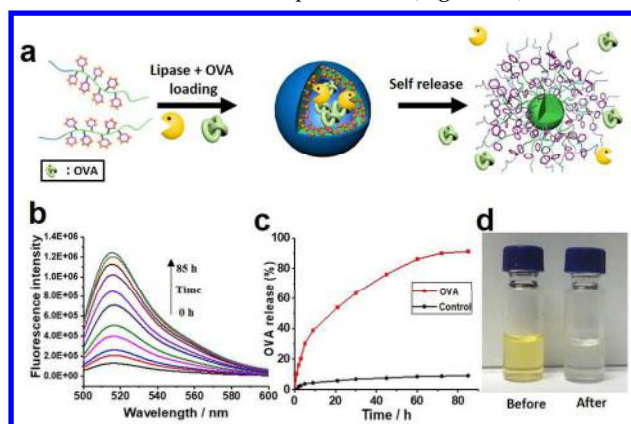
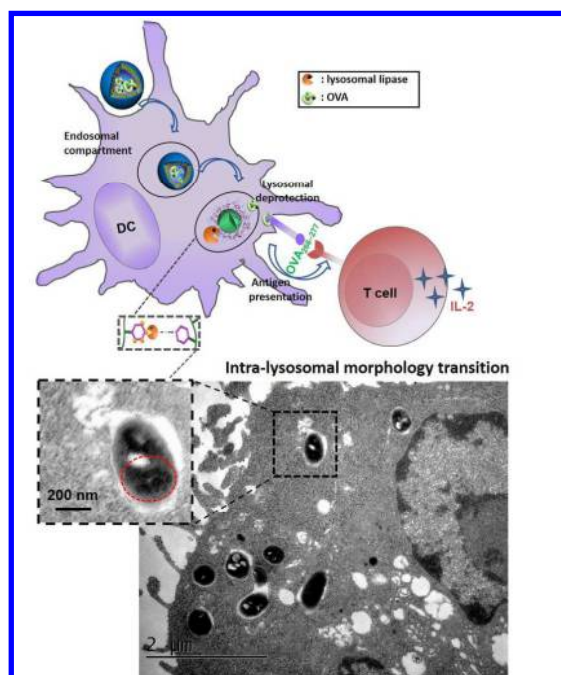


**Figure 6.** (a) Lipase-triggered release of OVA from glyco-vesicles. (b) Time-dependent fluorescence intensity at 519 nm increased gradually during the release of OVA. (c) Release profile (%) of OVA at pH 7.4 and 37 °C. Control: Without lipase loading. (d) Images of glyco-vesicles in aqueous solutions before (yellow) and after (colorless) the release of OVA. (FITC-labeled OVA was used in the experiments for fluorescence analysis)

**Enhanced cellular uptake and antigen presentation with lysosomal lipase as trigger.** Considering the abundance of lipases in lysosome which may catalyze the deprotection of glyco-vesicles,<sup>26</sup> lipase was not loaded into the glyco-vesicles in advance for cellular study. Thus the activation of glyco-vesicles in vitro was triggered by lysosomal lipase instead of the lipase from wheat germ we just used. The activation of the OVA-loaded glyco-vesicles via deprotection was examined by the efficiency of antigen presentation. Antigen presentation participates in many vital processes in the immune system including activation of helper T cells and cytotoxic T cells. Dendritic cells are the most effective antigen-presenting cells with the function of processing and presenting foreign antigen materials, such as tumor antigen.<sup>27</sup> After cellular uptake of foreign antigens, DCs display small peptides coupled with major histocompatibility complexes (MHCs) on their surfaces, which will trigger the activation of T cells.

**Scheme 3. Illustration of the endocytosis of OVA-loaded glyco-vesicles and antigen presentation by DC2.4 cells triggered by lysosomal lipase.**



To demonstrate the activation of the glyco-vesicles after deprotection *in vitro*, OVA-loaded glyco-vesicles were incubated with DCs, then lysosomal lipases of DCs triggered the deprotection of glyco-vesicles and the release of OVA afterwards. OVA-loaded glyco-vesicles were uptaken by DC2.4 cell line and presented to OVA<sub>266-277</sub> specific Ob4 hybridoma T cells. Interleukin 2 (IL-2) secretion by Ob4 cells was evaluated to indicate the efficiency of antigen presentation (Scheme 3). As mentioned in the previous reports<sup>28</sup>, cellular uptake of foreign antigens is mainly through the endosome-lysosome pathway. The TEM images of lysosomes within the DCs showed that the protected glyco-vesicles transformed into micelle-like structures (red circle) after lysosomal lipase catalyzed deprotection.

By flow cytometry analysis in Figure 7a, it was found that the cellular uptake of OVA was enhanced by its encapsulation in glyco-vesicles when compared to free OVA or, OVA/Glyco-vesicle mixture and OVA/Glyco-micelle mixture (Glyco-micelle was prepared by the deprotection of vesicles). To further evaluate the contribution of glyco-vesicles, these OVA-loaded DC2.4 cells were co-cultured with Ob4 cells for 72 h. As shown in Figure 7b, OVA-loaded glyco-vesicles stimulated a significant increase in IL-2 secretion compared to the free OVA group and the control groups (DC2.4 cells and Ob4 cells, OVA/Glyco-vesicle mixture and OVA/Glyco-micelle mixture). This result indicated that the deprotection of glyco-vesicles worked quite well in DCs triggered by lysosomal lipase, which not only released OVA but also exposed free sugars on the particle surfaces. Then the antigen and sugars worked together and stimulated T cells more efficiently than free OVA did, as a result of the enhanced antigen processing and presentation.

**Efficient Immune cell maturation by glyco-vesicle.** To confirm the glyco-vesicles themselves in the contribution to activate innate immune cells maturation, they were incubated with DC2.4 cells together without any antigen. It was found that after uptake and deprotection, the glyco-vesicles have a comparative boost effect as the deprotected glyco-

micelles. The maturation of DC2.4 cells was greatly promoted with significant upgraded expression of CD86 and I-A<sup>b</sup> (Figure 7c). Collectively, these results highlighted that glyco-vesicles worked together with loaded antigen, because of their "activation" during the enzymatic drug release process, indicating a novel type of nontoxic and intelligent vehicle with a novel adjuvant function for antigen delivery.

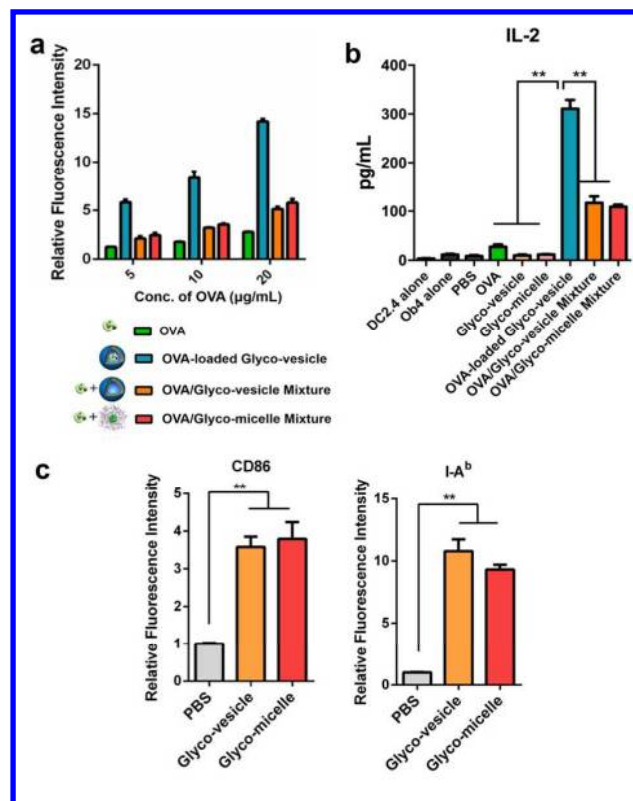


**Figure 7.** (a) Cellular uptake efficiency of free OVA, OVA-loaded Glyco-vesicle, OVA/Glyco-vesicle mixture and OVA/Glyco-micelle mixture after 24 h incubation. (FITC-labeled OVA was used in the experiment for fluorescence analysis) (b) IL-2 secretion by Ob4 cells was detected by ELISA to indicate the efficacy of antigen presentation. (c) Expression of CD86 and I-A<sup>b</sup> in Dendritic cell maturation assay. Mean  $\pm$  SEM, \*  $p < 0.05$ , \*\*  $p < 0.01$ .

## CONCLUSIONS

In summary, deprotection-induced glycopolymer assembly with antigen release was achieved by enzymatic trigger for the first time to the best of our knowledge. Lysosomal lipase was found to be an effective trigger, indicating no external lipase is needed for biological applications in this strategy. As designed in our glyco-vehicles, the PEG corona might ensure long circulation in the body while sugars were pre-protected to avoid unnecessary immune activation before arriving in lysosome. After lysosomal deprotection, the glyco-vehicle was re-activated and worked perfectly with the released antigen, showing the dual functions, delivery vehicle and immune adjuvant, of glyco-vesicles with protected glycopolymers as a novel design of responsive polymersomes. The effi-

cient improvement of antigen uptake and presentation to T cells by DCs indicated that the protected glyco-vesicles have a promising future in immunotherapy as well as delivery system. Finally considering acylation is a common type of modification to biomolecules, one may expect a bright outlook in the biological studies of this deacylation-induced morphology transition strategy.

## ASSOCIATED CONTENT

### Supporting Information.

The Supporting Information is available free of charge on the ACS Publications website at DOI: 10.1021/jacs.XXXXXXX.

Experimental details and characterization of synthesized glycopolymers and the corresponding precursors, including <sup>1</sup>H NMR, FTIR and SEC results, Experimental details of polymersome preparation and deprotection, TEM, UV-vis spectra for release study, cytotoxicity assay of glyco-vesicles (PDF)

## AUTHOR INFORMATION

### Corresponding Author

\* E-mail: guosong@fudan.edu.cn  
ORCID: 0000-0001-7089-911X

### Funding Sources

National Natural Science Foundation of China (Nos. 51721002, 1504016 and 91527305)

### Notes

The authors declare no competing financial interest.

## ACKNOWLEDGMENT

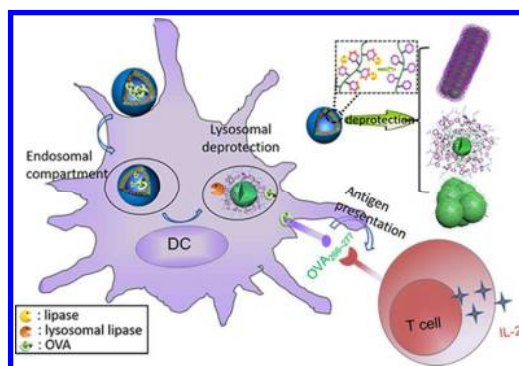
We acknowledge the financial support from the National Natural Science Foundation of China (Nos. 51721002, 21504016, and 91527305). We thank Joint Lab for Structural Research at the Integrative Research Institute for the Sciences (IRIS Adlershof, Berlin) for Cryo-TEM imaging.

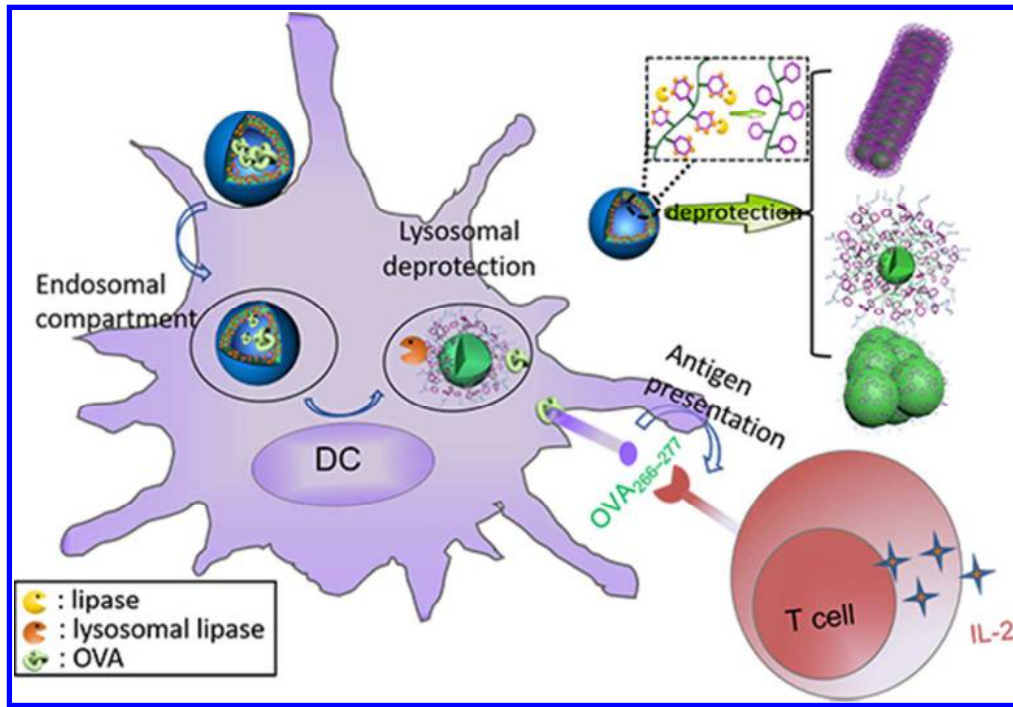
## REFERENCES

- Schoonen, L.; Hest, J. C.M.V. *Adv. Mater.* **2016**, *28*, 1109-1128.
- (a) Mable, C.; Derry, M. J.; Thompson, K. L.; Fielding, L. A.; Mykhaylyk, O. O.; Armes, S. P. *Macromolecules* **2017**, *50*, 4465-4473. (b) Qiao, Y.; Li, M.; Booth, R.; Mann, S. *Nat. Chem.* **2017**, *9*, 110-119.
- Figg, C. A.; Simula, A.; Gebre, K. A.; Tucker, B. S.; Haddleton, D. M.; Sumerlin, B. S. *Chem. Sci.* **2014**, *6*, 63-80.

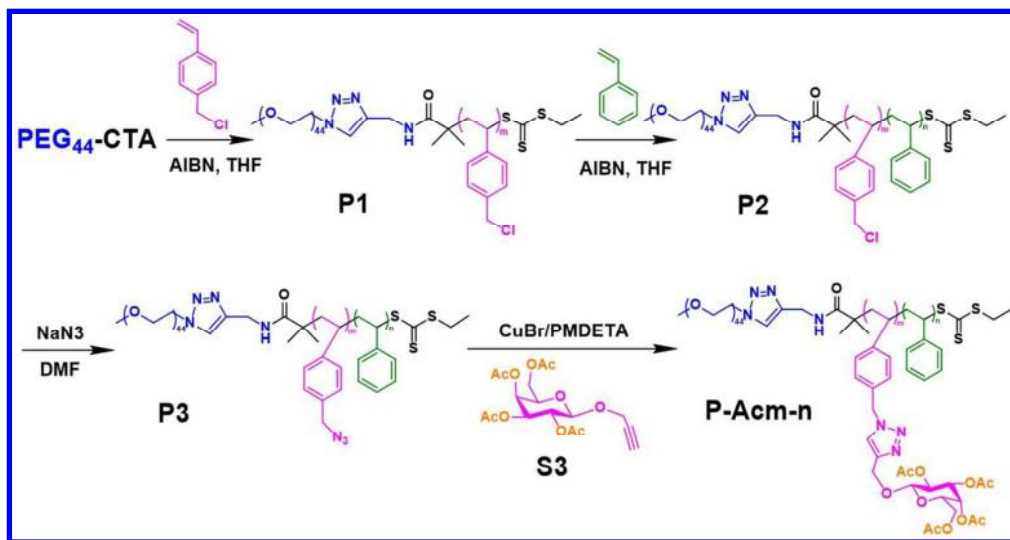
- Wang, X.; Hu, J.; Liu, G.; Tian, J.; Wang, H.; Gong, M.; Liu, S. *J. Am. Chem. Soc.* **2015**, *137*, 15262-15275.
- Schacher, F. H.; Elbert, J.; Patra, S. K.; Yusoff, S. F.; Winnik, M. A.; Manners, I. *Chem. Eur. J.* **2012**, *18*, 517-525.
- Chen, W.; Du, J. *Sci. Rep.* **2013**, *3*, 2162-2170.
- Rhee, P. G. V.; Rikken, R. S. M.; Abdelmohsen, L. K. E. A.; Maan, J. C.; Nolte, R. J. M.; Hest, J. C. M. V.; Christianen, P. C. M.; Wilson, D. A. *Nat. Commun.* **2014**, *5*, 5010-5017.
- Deng, Z.; Qian, Y.; Yu, Y.; Liu, G.; Hu, J.; Zhang, G.; Liu, S. *J. Am. Chem. Soc.* **2016**, *138*, 10452-10466.
- Tu, Y.; Peng, F.; White, P. B.; Wilson, P. D. A. *Angew. Chem. Int. Ed.* **2017**, *56*, 7620-7624.
- Wang, H.; Feng, Z.; Wu, D.; Fritzsche, K. J.; Rigney, M.; Jie, Z.; Jiang, Y.; Schmidtrohr, K.; Bing, X. *J. Am. Chem. Soc.* **2016**, *138*, 10758-10761.
- Li, J.; Kuang, Y.; Shi, J.; Zhou, J.; Medina, J. E.; Zhou, R.; Yuan, D.; Yang, C.; Wang, H.; Yang, Z. *Angew. Chem. Int. Ed.* **2015**, *54*, 13307-13311.
- Bertozzi, C. R.; Kiessling, L. L. *Science* **2001**, *291*, 2357-2364.
- Wu, L.; Zhang, Y.; Li, Z.; Yang, G.; Kochovski, Z.; Chen, G.; Jiang, M. *J. Am. Chem. Soc.* **2017**, *139*, 14684-14692.
- Zhang, Q.; Su, L.; Collins, J.; Chen, G.; Wallis, R.; Mitchell, D. A.; Haddleton, D. M.; Becer, C. R. *J. Am. Chem. Soc.* **2014**, *136*, 4325-4332.
- (a) Su, L.; Wang, C.; Polzer, F.; Lu, Y.; Chen, G.; Jiang, M. *ACS Macro Lett.* **2014**, *3*, 534-539. (b) Wu, X.; Su, L.; Chen, G.; Jiang, M. *Macromolecules* **2015**, *48*, 3705-3712.
- Penfold, N.; Lovett, J. R.; Verstraete, P.; Smets, J.; Armes, S. P. *Polym. Chem.* **2016**, *8*, 272-282.
- Skop, V.; Cahová, M.; Papáčková, Z.; Páleníčková, E.; Daňková, H.; Baranowski, M.; Zabielski, P.; Zdychová, J.; Zidková, J.; Kazdová, L. *Physiol. Res.* **2012**, *61*, 287-297.
- Carroux, C. J.; Rankin, G. M.; Moeker, J.; Bornaghi, L. F.; Katneni, K.; Morizzi, J.; Charman, S. A.; Vullo, D.; Supuran, C. T.; Poulsen, S. A. *J. Med. Chem.* **2013**, *56*, 9623-9634.
- hang, L. F.; Eisenberg, A. *J. Am. Chem. Soc.* **1996**, *118*, 3168-3181.
- Du, J.; Willcock, H.; Patterson, J. P.; Portman, I.; O'Reilly, R. K. *Small* **2011**, *7*, 2070-2080.
- Moughton, A. O.; O'Reilly, R. K. **2010**, *46*, 1091-1093.
- Fuente, J. M. D. L.; Penadés, S. *Glycoconj. J.* **2004**, *21*, 149-163.
- Reynolds, A. J.; Haines, A. H.; Russell, D. A. *Langmuir* **2006**, *22*, 1156-1163.
- Resh, M. D. *Nat. Chem. Biol.* **2006**, *2*, 584-590.
- Rajeshwara, A. N.; Prakash, V. *Chem. Biol. Drug. Des.* **1994**, *44*, 435-440.
- Monika, C.; Helena, D.; Eliska, P.; Zuzana, P.; Radko, K.; Jana, Z.; Eva, S.; Ludmila, K. *Biochem. Res. Int.* **2012**, *2012*, 135723-135733.
- Palucka, K.; Banchereau, J. *Nat. Rev. Cancer.* **2012**, *12*, 265-277.
- Lin, M.; Zhang, Y.; Chen, G.; Jiang, M. *Small* **2016**, *45*, 6065-6070.

## TOC

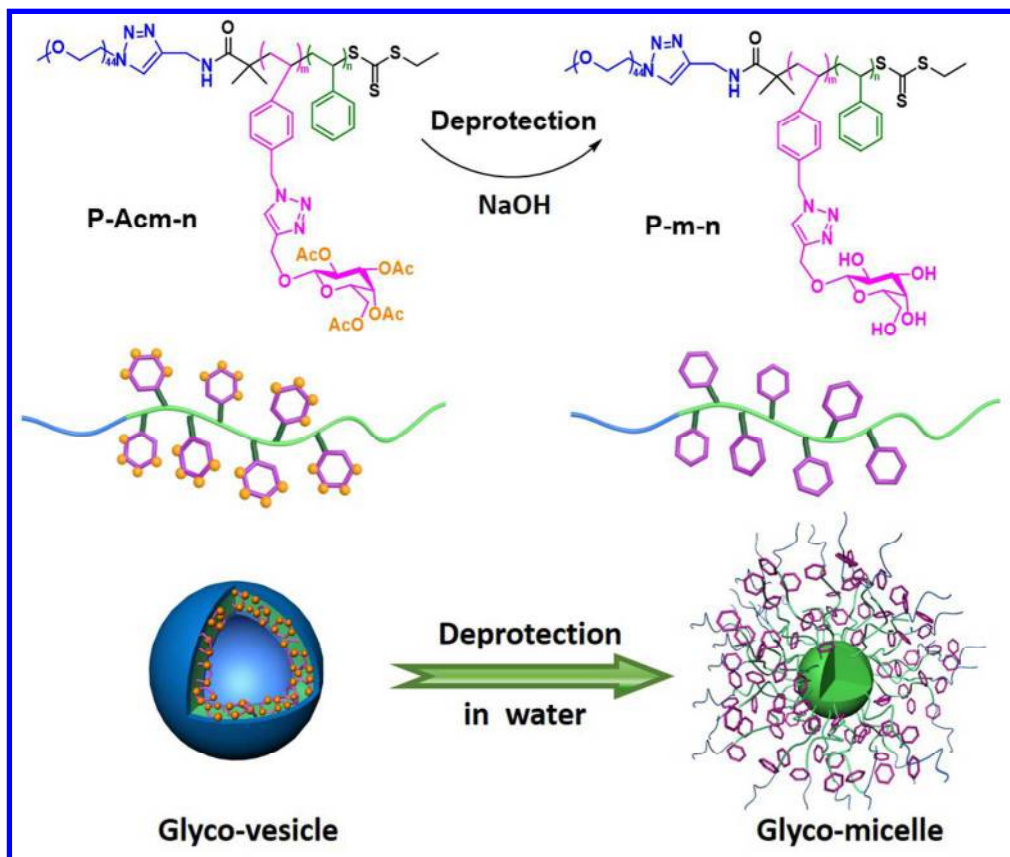




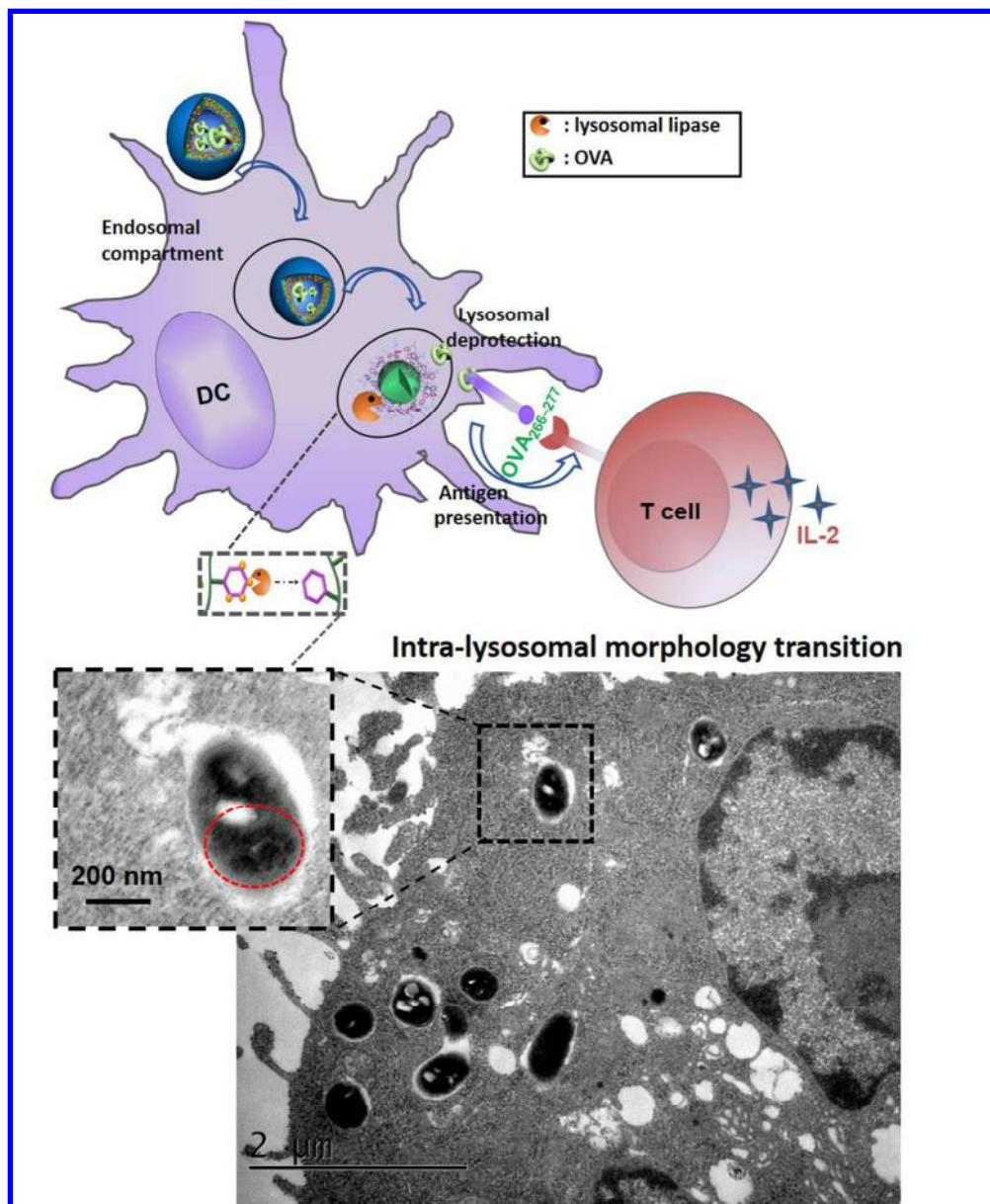
69x47mm (300 x 300 DPI)



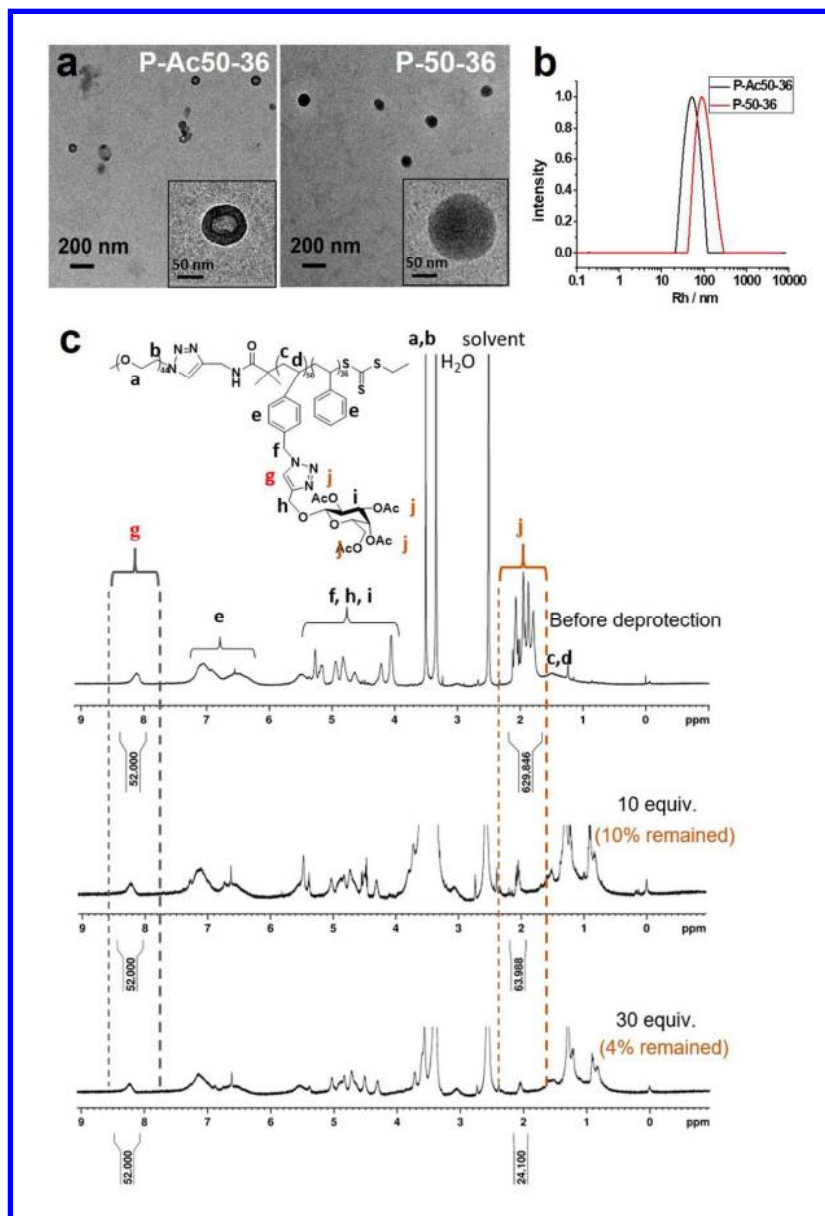
104x54mm (300 x 300 DPI)



94x79mm (300 x 300 DPI)



96x116mm (300 x 300 DPI)



106x156mm (300 x 300 DPI)

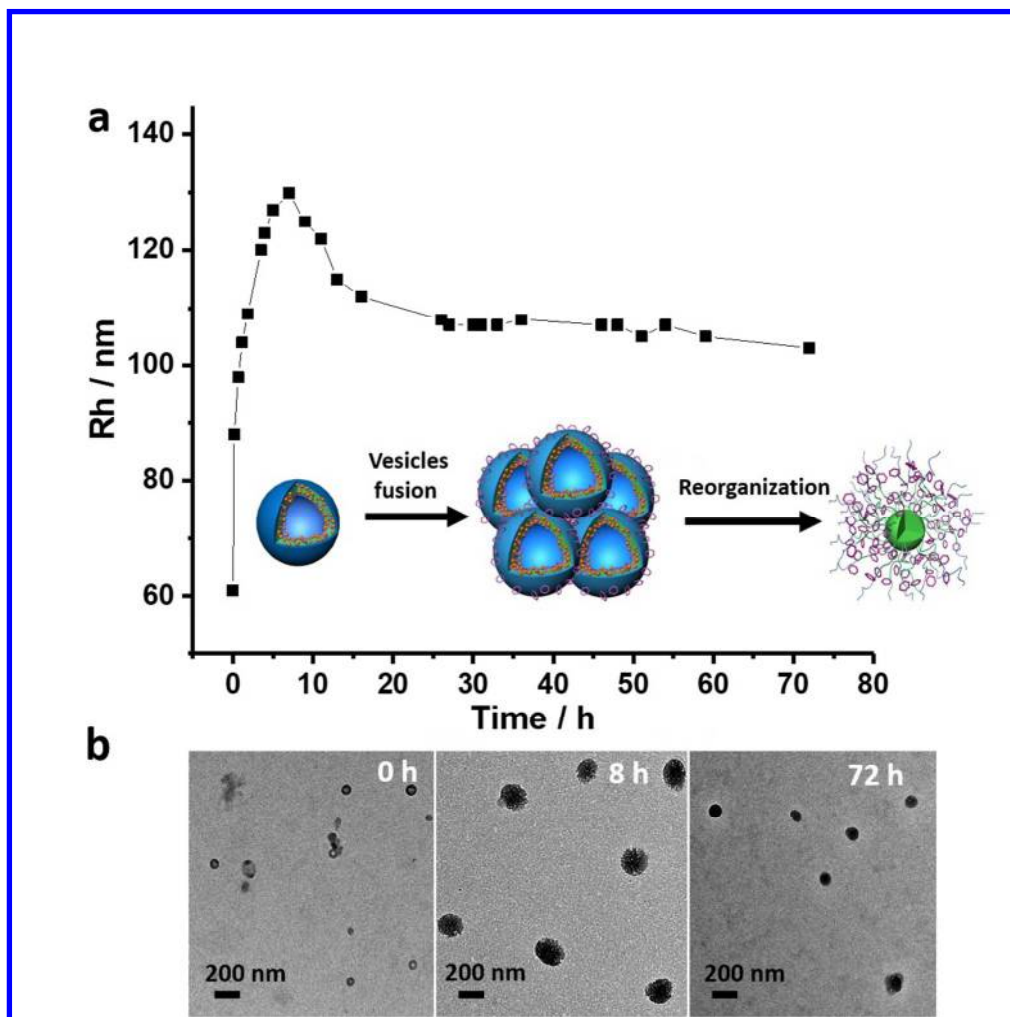
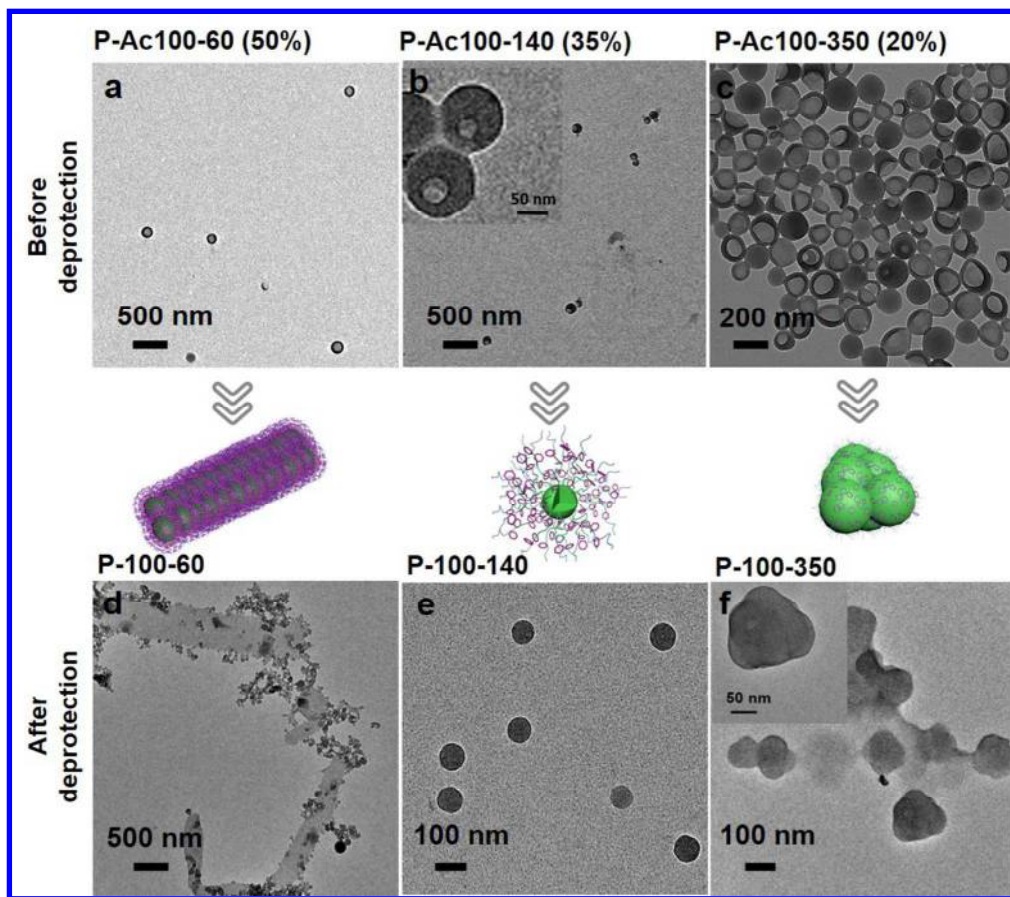
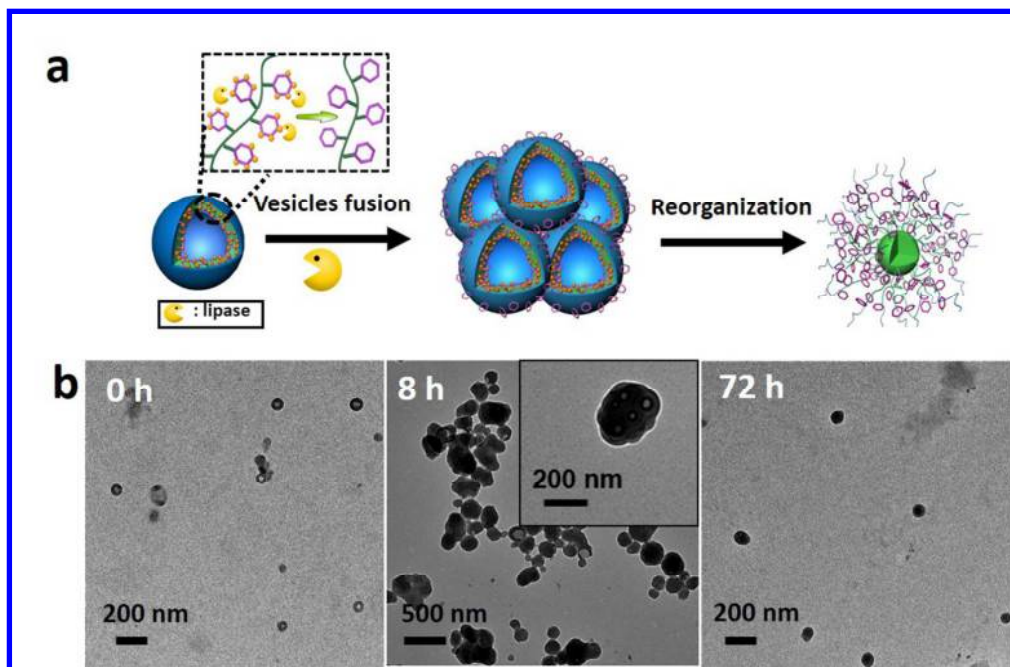


Figure 2

201x201mm (150 x 150 DPI)



94x82mm (300 x 300 DPI)



94x61mm (300 x 300 DPI)

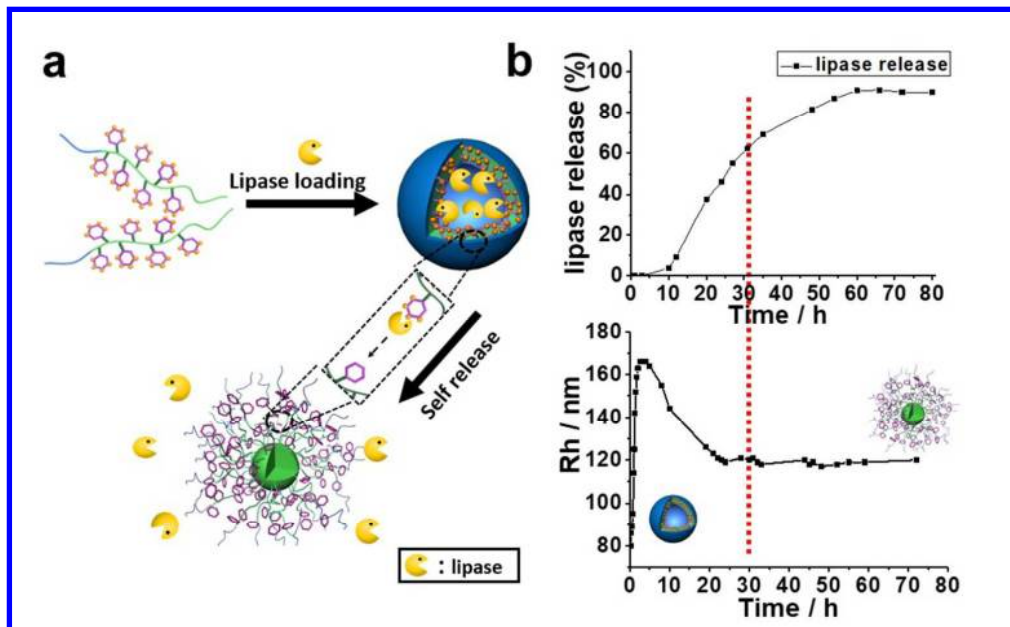


Figure 5

183x111mm (150 x 150 DPI)

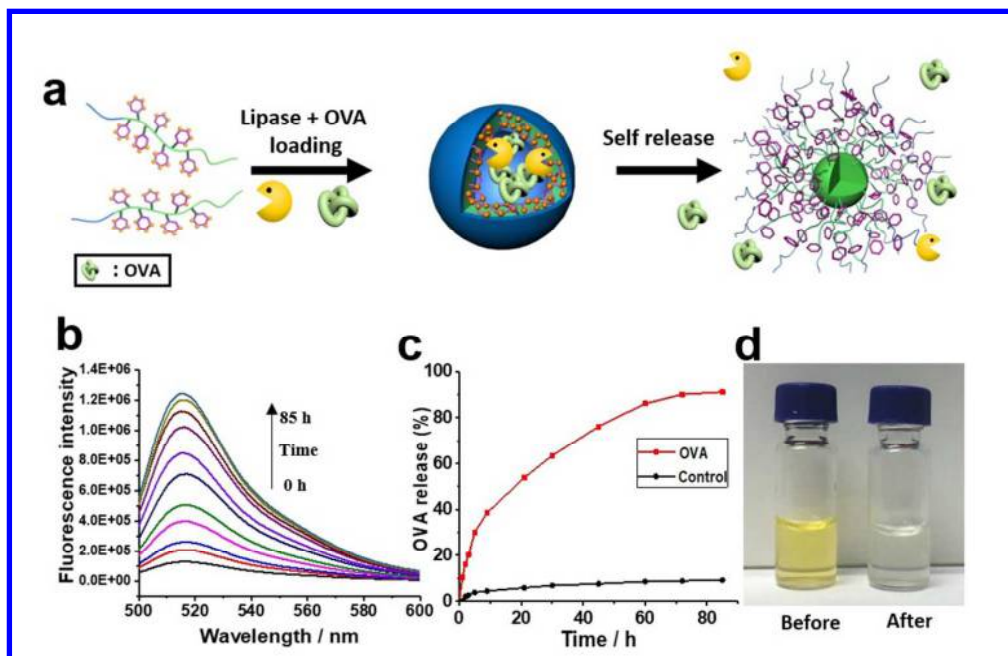
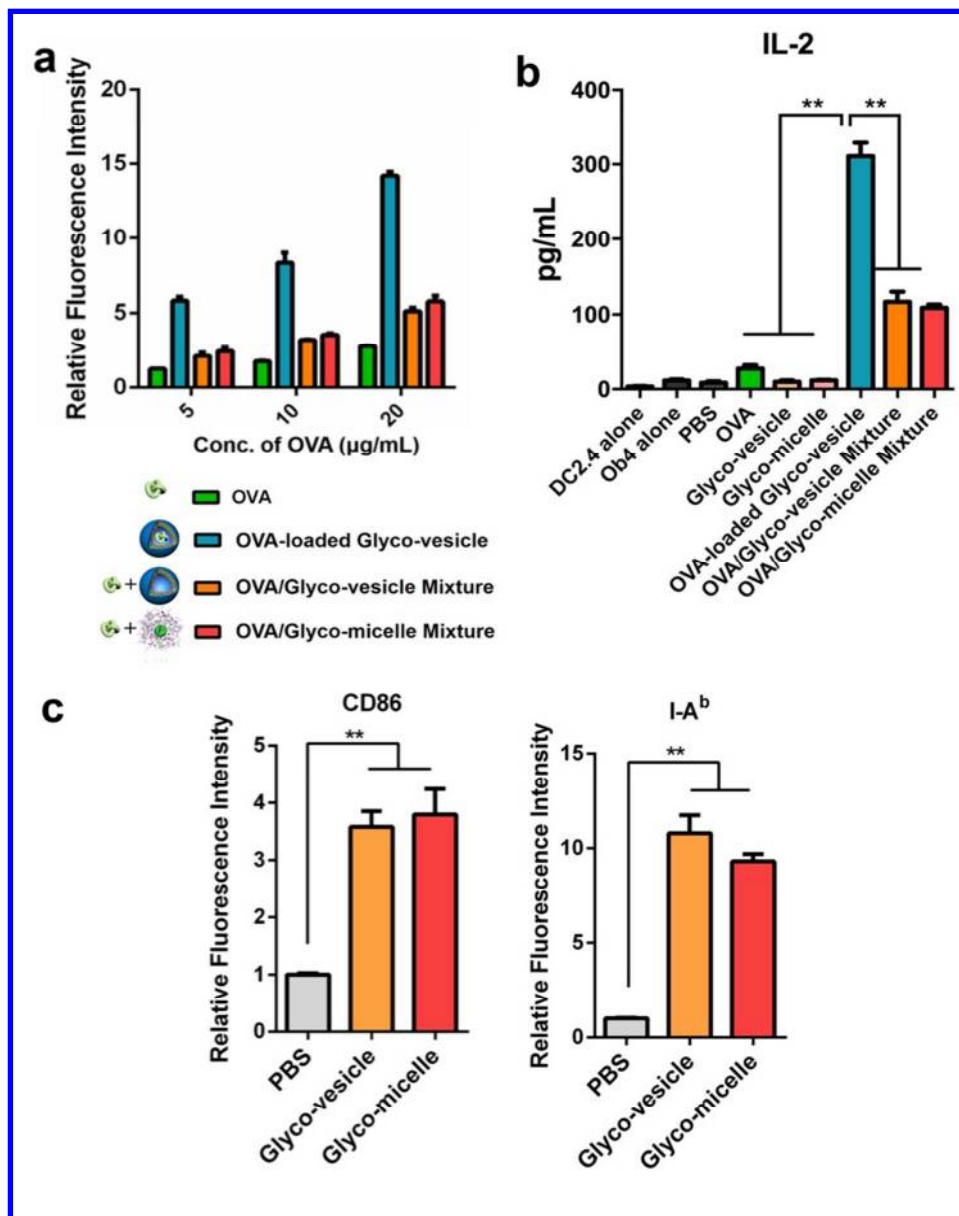


Figure 6

179x114mm (150 x 150 DPI)



155x196mm (150 x 150 DPI)